

Comparing transition-edge sensor response times in a modified contact scheme with different support beams

A.D. Beyer, M. E. Kenyon, B. Bumble, M. C. Runyan, P.E. Echternach, W.A. Holmes, J.J. Bock, and C. M. Bradford

Jet Propulsion Laboratory, California Institute of Technology, 4800 Oak Grove Dr., Pasadena, CA, USA

We present measurements of the thermal conductance, G , and effective time constants, τ , of three transition-edge sensors (TESs) populated in arrays operated from 80-87mK with $T_C \sim 120\text{mK}$. Our TES arrays include several variations of thermal architecture enabling determination of the architecture that demonstrates the minimum noise equivalent power (NEP), the lowest τ , and the trade-offs among designs. The three TESs we report here have identical Mo/Cu bilayer thermistors and wiring structures, while the thermal architectures are: 1) a TES with straight support beams of 1mm length, 2) a TES with meander support beams of total length 2mm and with 2 phonon-filter blocks per beam, and 3) a TES with meander support beams of total length 2mm and with 6 phonon-filter blocks per beam. Our wiring scheme aims to lower the thermistor normal state resistance R_N and increase the sharpness of the transition $\alpha = d\log R/d\log T$ at the transition temperature T_C . We find an upper limit of α given by (25 ± 10) , and G values of 200fW/K for 1), 15fW/K for 2), and 10fW/K for 3). The value of α can be improved by slightly increasing the length of our thermistors.

PACS numbers: 85.25.Pb; 95.85.-e; 85.25.-j

1. INTRODUCTION

To unravel the intricacies of the cosmic infrared background and to probe galaxies back to the first billion years, we have proposed the space-borne instrument known as the Background Limited Infrared/Sub-mm Spectrograph (BLISS) as an add on to the SAFARI instrument on the JAXA-led SPICA mission or as its own instrument on the Millimetron mission led by the Astro Space Center of Lebedev Physical Institut RAS. BLISS is a background-limited, broadband grating spectrometer with a resolving power of $R = \lambda/\Delta\lambda \sim 500$, is designed to achieve a sensitivity of 10^{-21} W/m^2 for the Millimetron mission, and will cover ~ 35 to $435\mu\text{m}$. To achieve the desired sensitivity, the detectors on BLISS must demonstrate noise equivalent power

A.D. Beyer et. al.

(NEP) $<10^{-19}$ W/Hz^{1/2} and be fast enough to optically chop the signal from 1 to 5Hz, implying an effective time constant $\tau < 160$ ms.

2. BLISS ARRAY ARCHITECTURE

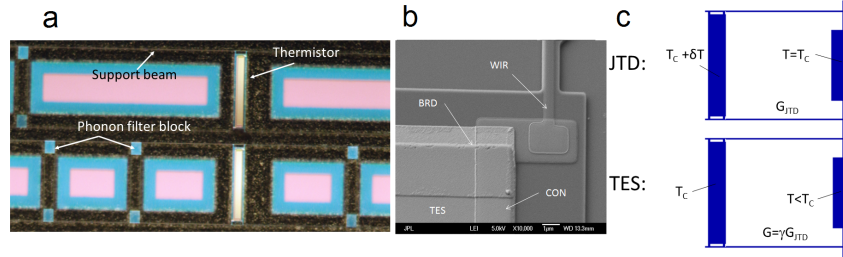


Fig. 1: a) Optical images of two TESs from a BLISS array. The Mo/Cu bilayer thermistor, silicon nitride (SiN) support beams, and phonon-filter blocks are shown. The top device has 2 phonon-filter blocks per beam, while the bottom device has 6 phonon-filters per beam. The SiN is pink in the image and the undercut from XeF₂ etching gives a blue color here. b) The contact structure for our TESs consists of a separate contact (CON) pad made of Ti with $T_c = 0.5$ K, a TiN wiring (WIR) layer with $T_c \sim 3.8$ K, and a gold border (BRD) layer to eliminate shorts on the edges of the Mo/Cu bilayer thermistor (TES). c) A schematic comparing Johnson noise Thermometry Devices (JTDs) and TESs when measuring thermal time constants $\tau_0 = C/G$, where C is the membrane plus metal film heat capacity. The schematics show the thermistor membrane on the left side at a temperature elevated above that of the substrate on the right at temperature T .

In Fig. 1a and b, we show two BLISS thermal architectures and the electrical wiring scheme employed¹. The arrays measured here consisted of 1 x 32 elements with varying support beam structures and membrane structures. One array had straight beam TESs with lengths of 0.1mm, 0.5mm, and 1mm, as well as 2mm meander beams. The membranes consisted of the thermistor platform alone or the thermistor platform plus a ladder-like structure resembling the BLISS absorbers. The other array had meander beam supports at right angles or in a diagonal fashion¹. In addition, some support beams had blocks dispersed along their length to add as phonon-filters to lower the thermal conductance G (see Fig. 1a). Only the thermistor support structures were used as membranes in the second 1 x 32 array. The electrical wiring scheme is the same among all TESs considered, and is designed to reduce unwanted proximity effects^{2,3}.

Comparing transition-edge sensor response times in a modified contact scheme with different support beams

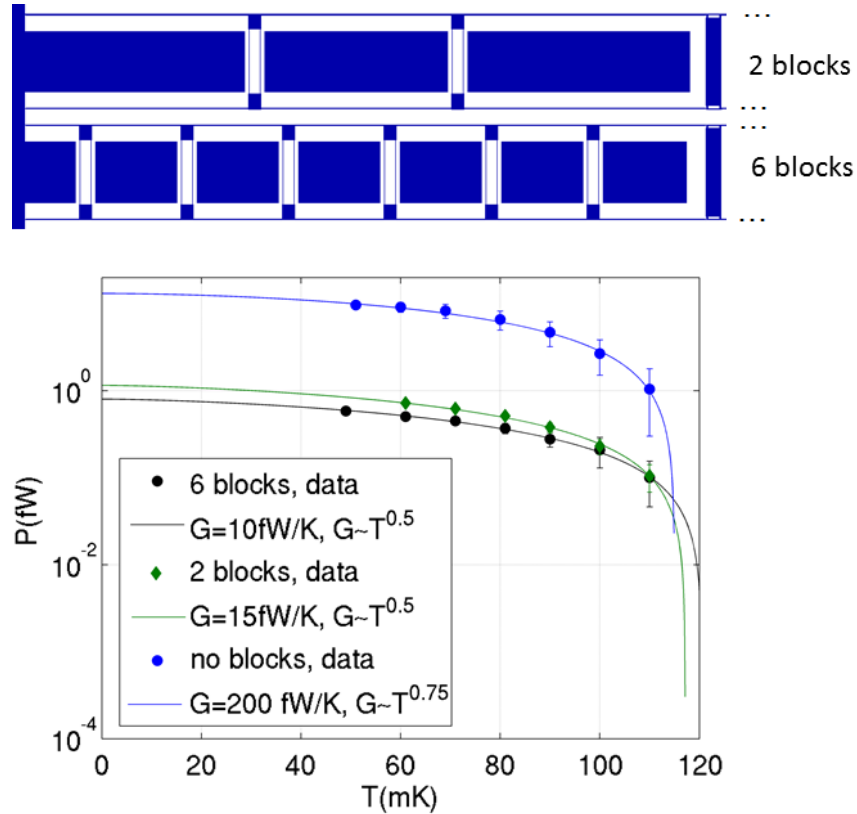


Fig.2 Top: Schematics of two support beam structures considered here, with 2 phonon-filter blocks per beam and 6 phonon-filter blocks per beam shown. Also considered is a beam without phonon-filter blocks and with straight beams instead of meander beams. Bottom: Power vs. substrate temperature curves for determining the thermal conductance for TESs with 2mm meander beams and 6 phonon filters per beam or 2 phonon-filters per beam, as well as 1mm long straight beams.

The expected NEP from such membrane-isolated TESs is predicted to follow $NEP = \sqrt{4k_B T_C^2 \gamma G}$, where k_B is Boltzmann's constant, $\gamma = (n+1)/(2n+3) \times (1-t^{2n+3})/(1-t^{n+1})$ with $t=T/T_C$ and G varying like $G \sim T^n$. Here, the γ term accounts for the thermal gradient along the beam when operating a TES with the membrane at T_C and substrate at $T < T_C$. The

formula for γ was derived in [4] for straight beams. Previously, we have measured the thermal conductance of Johnson noise Thermometry Devices (JTDs)⁵ to predict the NEP and τ of our TESs. In those measurements, γ is not used to estimate τ_0 . To estimate the speed up of devices, we consider $\tau_0=C/G$ and $\tau_0=C/(\gamma G)$ as the lower and upper limits of τ_0 to determine the effectiveness of electrothermal feedback in lowering τ .

3. RESULTS AND DISCUSSION

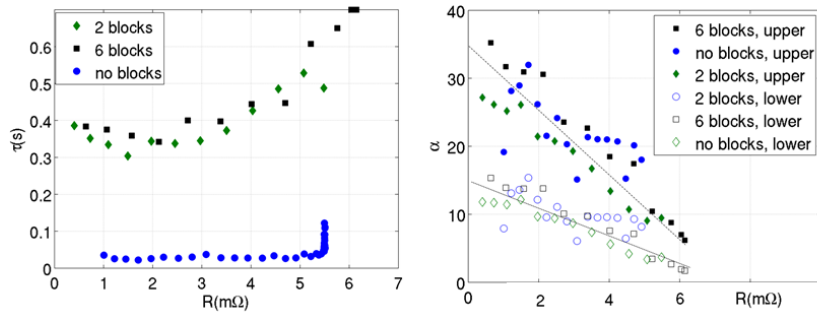


Fig.3 Left: The effective time constants τ as measured within the transition for the TESs with no phonon-filter blocks (at 80mK), 2 phonon-filters per beam (at 87mK), and 6 phonon-filters per beam (at 87mK). Right: The upper and lower limits of α within the transition of all three devices. The lines are guides to the eye. Given the shape of the R vs. T transitions we have observed, we expect α to be approximately constant in different parts of the transition so that the assumption of $\beta=0$ is likely not valid here. Nevertheless, the comparison and consistency of α demonstrates a reliable contact structure.

In contrast to the situation in electrothermal feedback TESs⁶, JTDs are typically operated with the substrate temperature T nearly equal to that at the membrane, $T+\delta T$. As shown in Fig. 1c, the G measured by a JTD would be expected to be γ times smaller in TES operation. The improvement in effective time constant due to the sharpness of the transition $\alpha=d\log R/d\log T$ is expected to follow $\tau=\tau_0 \times 1/[1+P_J\alpha/(GT_C)]$, where P_J is the Joule power used to bias the thermistor within the transition region at T_C and C is the heat capacity of the membrane. The values of G obtained by fitting P_J vs. T curves are shown in Fig.2 for: 1) a TES with straight support beams of 1mm length, 2) a TES with meander support beams of total length 2mm and with

Comparing transition-edge sensor response times in a modified contact scheme with different support beams

2 phonon-filter blocks per beam, and 3) a TES with meander support beams of total length 2mm and with 6 phonon-filter blocks per beam. G is 200fW/K for 1), 15fW/K for 2) and 10 fW/K for 3). The value of G does not simply scale with length so that either G is reduced by the added phonon-filters or the analytical formula for γ is not valid for such support beams.

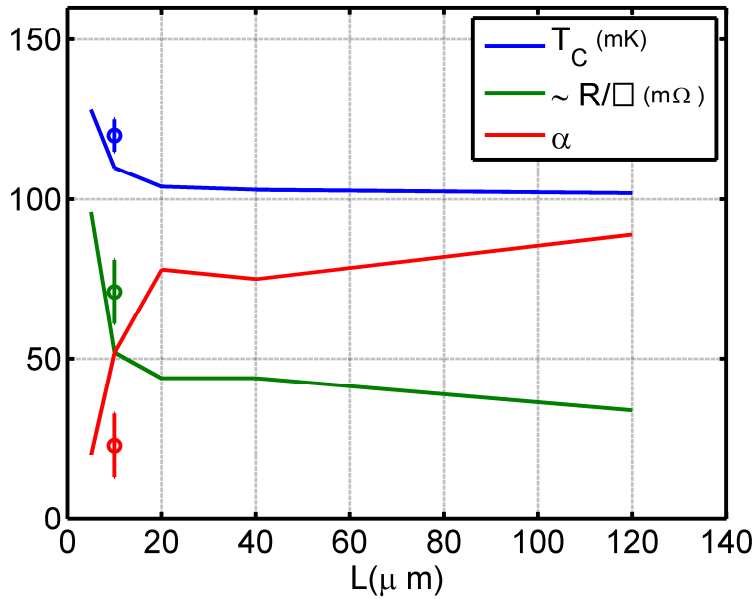


Fig.4: A comparison of values for T_C , α , and R/sq obtained from the Mo/Cu bilayer thermistors measured here (symbols with error bars) to that of test thermistors with the same CON/WIR scheme tested in [1] and with varying lengths (solid lines). The thermistors were designed to be 10 μm in length in the arrays considered here, but it appears as though the effective length is slightly shorter, ~ 7 to 8 μm .

The analysis for τ considered here assumes that $\beta = d\log R/d\log I = 0$, which is not usually valid throughout the TES operating range. Here, assuming $\beta = 0$ is a simple starting point to analyze α in BLISS TESs. Using this conjecture, we may say $\alpha \approx (\tau_0/\tau - 1) \times GT_C/P_J$ throughout the transition at T_C from R_N to $R \sim 0$, where R_N is the normal state resistance of the thermistor. Assuming a lower limit for $\tau_0 = C/G$ and an upper limit of $\tau_0 = C/(\gamma G)$, we

A.D. Beyer et. al.

show the approximate upper and lower limits for α throughout the transition of the three TESs considered here with $R_N \approx 6m\Omega$. We find from this analysis that the maximum of $\alpha=(25\pm 10)$. One would expect constant values of α or piece-wise constant values, implying that $\beta=0$ is not a valid assumption. However, the consistency among devices is as expected, and further analysis of β could be used to compare the RSJ and two-fluid models⁷.

Finally, the results are summarized in Fig.4 and compared with data taken from [1], where Mo/Cu thermistors of varying lengths and Ti contacts were measured. In our design, the thermistor length is ideally $10\mu m$. The values found for T_C , α , and R/\square approximately agree with those found previously. By inferring that the effective length is slightly shorter than designed, the values would fall on those previously measured in [1]. In order to more fully take advantage of the increase in α afforded by the separate WIR/CON scheme, we should slightly increase the design length of our TESs to $\sim 20\mu m$. The sharp increase in α for slightly longer devices would speed the devices up by a factor of 2 to 3 leading to improved bandwidth. Additionally, the uniformity of the array will likely be improved.

REFERENCES

1. A.D. Beyer, P.M. Echternach, M.E. Kenyon, M.C. Runyan, B. Bumble, C.M. Bradford, J.J. Bock, W.A. Holmes, *IEEE Trans. On Applied Superconductivity*, **23**, 2100104 (2013).
2. J.E. Sadleir, S.J. Smith, S.R. Bandler, J.A. Chervenak, and J.R. Clem, *Phys. Rev. Lett.* **104**, 047003 (2010).
3. J.E. Sadleir, S.J. Smith, I.K. Robinson, F.M. Finkbeiner, J.A. Chervenak, S. R. Bandler, M.E. Eckart, C.A. Kilbourne, *Phys. Rev. B*, **84**, 184502 (2011).
4. J.C. Mather, *Applied Optics*, **21**, 1125 (1982).
5. A.D. Beyer, M.E. Kenyon, P. M. Echternach, B.-H. Eom, J. Bueno, P.K. Day, J.J. Bock, and C.M. Bradford, *Proc. SPIE*, **7741**, 774121 (2010).
6. K.D. Irwin and G.C. Hilton, *Topics App. Phys.* **99**, 63 (2005).
7. D.A. Bennett, D.S. Swetz, D.R. Schmidt, J.N. Ullom, *Phys. Rev. B*, **87**, 020508 (2013).